6364–6374 *Nucleic Acids Research, 2021, Vol. 49, No. 11* *Published online 31 May 2021*
https://doi.org/10.1093/nar/gkab439

New DNA-hydrolyzing DNAs isolated from an ssDNA library carrying a terminal hybridization stem

Canyu Zhang[1,2], Qingting Li[1], Tianbin Xu[1], Wei Li[1], Yungang He[1] and Hongzhou Gu[1,2,*]

[1]Fudan University Shanghai Cancer Center, and the Shanghai Key Laboratory of Medical Epigenetics, Institutes of Biomedical Sciences, Shanghai Stomatological Hospital, Fudan University, Shanghai 200433, China and [2]Center for Medical Research and Innovation, Shanghai Pudong Hospital, Fudan University Pudong Medical Center, Shanghai 201399, China

Received March 26, 2021; Revised May 03, 2021; Editorial Decision May 04, 2021; Accepted May 06, 2021

ABSTRACT

DNA-hydrolyzing DNAs represent an attractive type of DNA-processing catalysts distinctive from the protein-based restriction enzymes. The innate DNA property has enabled them to readily join DNA-based manipulations to promote the development of DNA biotechnology. A major in vitro selection strategy to identify these DNA catalysts relies tightly on the isolation of linear DNAs processed from a circular single-stranded (ss) DNA sequence library by self-hydrolysis. Herein, we report that by programming a terminal hybridization stem in the library, other than the previously reported classes (I & II) of deoxyribozymes, two new classes (III & IV) were identified with the old selection strategy to site-specifically hydrolyze DNA in the presence of Zn^{2+}. Their representatives own a catalytic core consisting of ∼20 conserved nucleotides and a half-life of ∼15 min at neutral pH. In a bimolecular construct, class III exhibits unique broad generality on the enzyme strand, which can be potentially harnessed to engineer DNA-responsive DNA hydrolyzers for detection of any target ssDNA sequence. Besides the new findings, this work should also provide an improved approach to select for DNA-hydrolyzing deoxyribozymes that use various molecules and ions as cofactors.

INTRODUCTION

DNA phosphodiester bonds are extremely stable among the linkages of the three bio-macromolecules, DNA, RNA and proteins, with a half-life of spontaneous hydrolysis estimated to be million years (1–3). Selective hydrolysis of DNA bonds was commonly achieved through the ubiquitous protein-based restriction enzymes *in vivo* and *in vitro*, and was also considered as the privileges of protein enzymes for long lime. Until recently, the identification of DNA-hydrolyzing deoxyribozymes (4–13) not only broke that tradition and refreshed biochemists' cognition on DNA's catalytic ability, but also diversified the types of molecular tools for DNA editing, leading to a series of unique applications in DNA biotechnology (14–17). For example, massive amounts of various target ssDNAs for origami construction were biotechnologically produced through auto-processing of ssDNA amplicons via self-hydrolyzing DNAs; (15) anticancer drug molecules were precisely and efficiently delivered with DNA sponges carrying environment-responsive DNA-hydrolyzing DNAs (16). They have also shown great values in bio-sensing and nanotechnology (18–28).

All existing DNA-hydrolyzing DNAs are identified through *in vitro* selection from synthetic ssDNA libraries containing random sequence (4,7,10). Previously, the Breaker lab invented a powerful strategy that permits selection of DNA-catalyzed DNA hydrolysis at any location within individual ssDNAs in a sequence library (Figure 1, Pre) (10). This method relies on an enzyme named CircLigase to circularize DNAs twice in one round of selective amplification: the first (step i) is to turn a linear DNA library (145 nt) into circular, thus enabling the separation of self-hydrolyzed DNAs (linear) from un-cleaved ones (circular) in the following steps by denaturing polyacrylamide gel electrophoresis (dPAGE); the second (step v) is to religate the collected hydrolyzed DNAs (linear) back into circles as effective templates for PCR amplification to rebuild the library for next round of selection (Figure 1). Based on this strategy, two classes (I & II) of highly active deoxyribozymes had been identified to selectively hydrolyze DNA in the presence of Zn^{2+} (10), with a robust member (I-R3) of class I prevailing in several DNA-based manipulations (13–28). Due to their robustness, neatness, steadiness, and easiness-to-operation, more types of DNA-hydrolyzing DNAs are urgently needed by technology developers in order to satisfy various demands (13,22,24).

In the past decade, we and others applied this CircLigase-based strategy (10) to select for DNA-hydrolyzing DNAs that can use other metal ions (e.g. Cd^{2+}, Ni^{2+}, Co^{2+}) or amino acids as cofactors. However, those unpublished ef-

*To whom correspondence should be addressed. Tel: +86 021 54237322; Fax: +86 021 54237322; Email: hongzhou.gu@fudan.edu.cn

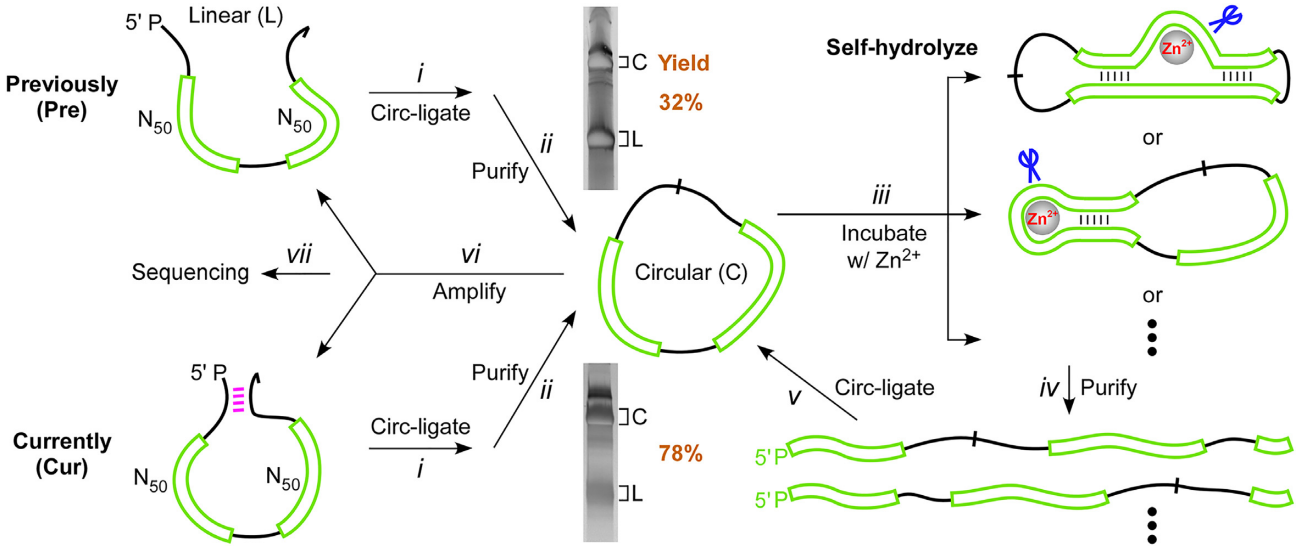

Figure 1. An in vitro selection scheme to identify DNA-hydrolyzing DNAs. N_{50} designates 50 random-sequence nucleotides. The current (Cur) ssDNA library contains designed terminal hybridization, while the library used in the previous (Pre) selection study (10) has no such secondary structure. With programmed terminal hybridization, the linear (L) DNA library was more efficiently (i) ligated by CircLigase into monomeric circular (C) DNAs, as shown by the (ii) dPAGE gels with a yield of 78% (Cur) over 32% (Pre). Unlabeled bands correspond to concatemeric byproducts generated during circularization (29). The purified circular DNA library was (iii) incubated in a selection buffer (Zn^{2+}) for potential self-hydrolysis. Cleaved DNAs were (iv) separated by dPAGE and (v) re-ligated with CircLigase to (vi) generate C-DNA templates for PCR amplification to rebuild the linear library for next round of selection. After a few rounds of selective amplification, the DNAs from this stage (vi) were also (vii) sequenced for further analysis. Note that presented here are gels to separate circularized products of the initial (G0) ssDNA library.

forts failed to yield such DNAs. As we looked back into the strategy, we realized that the circularization efficiency (32%) for the initial (G0) ssDNA library was relatively low (Figure 1, Pre), and the low yield of the first-step circularization lasted through the rounds (G0-G9) of the previous selection (Supplementary Figure S1, Pre) (10). We were a little worried about that the inefficiency in the initial (G0) circularization by CircLigase might had compromised the selection by limiting the number of unique DNA sequence in the library for interrogation, despite of the success in the isolation of the class I & II Zn^{2+}-dependent DNA-hydrolyzing deoxyribozymes (10). Besides, we noticed that by introducing secondary structures into a sequence library, one can enhance the library's functional potential and improve the selection outcome for aptamers (30), another kind of functional nucleic acid molecules that can evolve out of test tubes. Coincidentally, in a recent study (29) we found that the CircLigase-catalyzed DNA circularization can be robustly promoted (>75% yields) by programming 5′-3′ terminal hybridization in the linear ssDNA, which yields circular ssDNA products with a terminal stem. Considering the resulted double benefits|the improved circularization efficiency and the incorporation of a pre-determined secondary structure into circular ssDNA, we were very interested to see whether and how the terminal hybridization would affect the outcome of the CircLigase-based selection for DNA-hydrolyzing DNAs. Therefore we decided to reinvestigate the old selection (10) with a new ssDNA sequence library containing designed terminal complementation (Figure 1 & Supplementary Figure S1, Cur), which is supposed to generate more number of circular ssDNAs with a pre-existing stem substructure by CircLigase for selection.

MATERIALS AND METHODS

Oligonucleotides

The two half-libraries used to build the full-length 145-nt or 149-nt ssDNA library were ordered from Integrated DNA Technologies (IDT). All other oligonucleotides, including the full-length (149 nt) deoxyribozyme precursors chosen for analysis, truncated deoxyribozyme representatives with various lengths, and synthetic DNA markers for mapping cleavage site, were purchased from the Shanghai Generay Biotech Co. Ltd.

In vitro selection and isolation of self-hydrolyzing deoxyribozymes

The ssDNA library A (5′-pGTCCGTGCG CAGACCAA$(N)_{50}$GACTGCATCACGAAG) and library B (5′-GCTCGTGCGCAGACAG C$(N)_{50}$CTTCGTGATGCAGTrC) (underline refers to complementary nucleotides between A and B that were designed for primer extension; p: phosphate; N: nucleotide with random sequence) were purified by denaturing polyacrylamide gel electrophoresis (dPAGE), and then annealed in a standard PCR buffer for extension by Taq DNA polymerase. A ribonucleotide (rC) was designed at the 3′ terminus of library B to permit site-specific degradation of one template strand of the extension products by treatment with 0.25 M NaOH at 90°C for 5 min. The desired 149 nt ssDNA library products were separated from the unwanted and digested complementary strands by 8% dPAGE.

In subsequent rounds of selection, primer 1 (5′-pGTCCG TGCGCAGACCAA) and primer 2 (5′-GCTCGTGCGC AGACAGrC) were used to amplify the selected signal. A

rC was also included at the 3′ terminus of primer 2 to permit degradation of one template strand in dsDNA amplicons by treatment with NaOH, and the full-length 149-nt ssDNA products were again purified by 8% dPAGE.

To prepare circular ssDNA library for selection, ∼200 pmol of the 149-nt ssDNA library were used for circularization by CircLigase (EpiCentre) at 60°C for 2 h in the buffer containing 50 mM MOPS, 10 mM KCl, 2.5 mM $MgCl_2$, 2.5 mM $MnCl_2$, 0.05 mM ATP and 1 mM DTT. Circular DNAs were then purified by 8% dPAGE. Before incubating them in the selection buffer, DNAs containing abasic sites were removed by subjecting the circular DNAs in 0.1 M piperidine at 80°C for 30 min. Intact circular DNAs were recovered as the initial pool for selection by PAGE purification as described above.

Incubation of the DNA pool was performed in a selection buffer containing 50 mM HEPES, 100 mM NaCl, 5 mM $MgCl_2$ and 2 mM $ZnCl_2$ at 37°C for 1 h (as rounds of selection were going on, the incubation time was shortened later to minutes to select for deoxyribozymes with robust activities). Cleaved DNAs were separated by denaturing 8% PAGE and re-ligated by CircLigase back to circles (60°C, 2 h). These circular DNAs were purified by denaturing 8% PAGE, and used as templates for PCR amplification to rebuild the dsDNA library. One strand in the dsDNA contains a ribonucleotide that comes from the corresponding primer 2, and can be cleaved in the position by treatment with 0.25 M NaOH at 90°C for 5 min. The other strand, full-length and intact, was purified by 8% dPAGE to regenerate the ssDNA library for next round of selection. The G9 DNA population was picked up for high-throughput sequencing.

In vitro reselection

The initial ssDNA libraries for Zn-III and Zn-IV reselection were built on their corresponding representative Zn-III-R1 (5′-pGACGTGC TAGCGCAGACCAACGACTGCTTTTGCAGT CGTTTTTATGGACTGATCATGCCCTGCTGTCT GCGCTAGGCACCT) and Zn-IV-R1 (5′-pACCACGA CGAGTGCCGGCGTTGTGAGTGGTGACTGCTCC AGTTTTCTGGAGCAGTAACATGCCCGGCACTCG TGTACGG), respectively, with a degeneracy (31) of 0.18 at each underlined nucleotide (33 nt for Zn-III, and 29 nt for Zn-IV). In vitro reselection was performed using the same protocols described above in the session of *in vitro* selection.

Briefly, ∼200 pmol of the ssDNA pool (∼100 μl) were circularized by CircLigase (50–60°C, 2 h) and purified by 10% dPAGE. The purified products were treated with 0.1 M piperidine (80°C, 30 min), and the intact circular DNAs were separated by 10% dPAGE. Then the circular DNA pool was incubated in the selection buffer at 37°C for 60 min (30 min for G6, 5 min for G7 and G8). Cleaved DNAs were isolated by 10% dPAGE, and re-ligated by CircLigase (60°C, 2 h) to regenerate circular DNAs as templates for PCR amplification. The dsDNA amplicons were then treated with 0.25 M NaOH at 90°C for 5 min to digest the unwanted anti-sense strand. The wanted sense strand was purified by 10% dPAGE to rebuild the ssDNA library for next round of selection. The G4 DNA population was picked up for high-throughput sequencing. Clones (pMDTM18-T Vector Cloning Kit, Takara) from the G8 population were sequenced for further analysis.

Mapping the cleavage site of deoxyribozymes

About 16 pmol of candidate DNAs were incubated in 300 μl of the selection buffer at 37°C for 2–6 h. Then the samples were precipitated with ethanol (buffer versus ethanol: 1 versus 3, v/v), and re-dissolved in 40 μl of loading buffer (90% formamide, 30 mM EDTA, 0.025% bromophenol blue, 0.025% xylene cyanol). About 8 μl of the resuspended reaction products were loaded with a synthetic ssDNA marker on the 15% dPAGE gel for band-migration comparison.

Sample preparation for exact mass spectrometry

About 40 pmol of the substrate DNA and 50 pmol of the enzyme DNA were mixed in 400 μl solution containing the selection buffer (50 mM HEPES (pH 7.05 at 23°C), 100 mM NaCl, 5 mM $MgCl_2$, and 2 mM $ZnCl_2$), and incubated at 37°C for overnight. The products were precipitated with ethanol, dried at 37°C for 20 min, and resuspended in 10 μl ddH_2O before mass-spec characterization (Novatia).

Kinetic characterization of deoxyribozymes

All kinetic assays were performed with bimolecular DNA constructs. About 10 pmol of the 5′ FAM labeled substrate DNA strand and 30 pmol of enzyme DNA strand were mixed and incubated in 300 μl of the selection buffer at 37°C or a different temperature. At different time points of 0 s, 20 s, 40 s, 1 min, 2 min, 5 min, 10 min, 20 min, 40 min and 1h, 8 μl of the sample was pipetted out and mixed with 8 μl of the loading buffer (90% formamide, 30 mM EDTA, 0.025% bromophenol blue, 0.025% xylene cyanol) to stop the reaction. The collected samples were then run into a 13% dPAGE gel for bands separation. The fluorescence signal of DNA was detected by a Typhoon FLA9500 scanner. The information of fraction cleaved versus time was extracted from the gels for calculating the observed rate constant of each deoxyribozyme. Values for the observed rate constant k_{obs} were established by using the following equation: fraction cleaved $= FC_{max}(1 - e^{-kt})$, where $k = k_{obs}$ and FC_{max} = maximum of fraction cleaved.

Metal ion dependency of deoxyribozymes

Similar to the protocols used in kinetic characterization, a series of buffers (50 mM HEPES (pH 7.05 at 23°C), 100 mM NaCl) containing different divalent metal ions (2 mM) or different combination of divalent metal ions were prepared. To identify the dependence of Zn^{2+} concentration, the deoxyribozyme samples were incubated at 37°C in the reaction buffers containing various concentrations of Zn^{2+} (from 0.1 mM to 20 mM) for 20 min or 2 h. All reaction products were analyzed on 13% dPAGE gels.

pH dependency of deoxyribozymes

A series of buffers (50 mM HEPES, 100 mM NaCl, 5 mM $MgCl_2$ and 2 mM $ZnCl_2$) containing various pH values (from 6.85 to 7.55) were prepared. To identify the pH dependence, the deoxyribozyme samples were incubated at 37°C in these buffers for 20 min or 2 h. All reaction products were analyzed on 13% dPAGE gels.

Mutational analysis of Zn-III-R2

For each mutation or covariation, about 16 pmol of the substrate DNA strand and 48 pmol of the enzyme DNA strand were mixed in 50 μl of the selection buffer (50 mM HEPES (pH 7.05 at 23°C), 100 mM NaCl, 5 mM $MgCl_2$, and 2 mM $ZnCl_2$). The samples were incubated at 37°C for 1 h. All reaction products were then loaded on 15% dPAGE gels for bands separation. The gels were stained by SYBR Gold, scanned with a Bio-rad ChemiDoc MP Imaging System, and analyzed with the ImageQuant software.

Bacterial cell lysate preparation

The wild-type *Escherichia coli* was cultured at 37°C in 2 ml LB medium for about 10 h with continuous shaking at 220 rpm to yield a turbid suspension. Cells were then centrifuged at 5000 rpm for 10 min at 4°C. The supernatant was discarded, and the pellet was resuspended in 6 ml ddH_2O and heated at 100°C for 10 min to generate the lysate.

Programmed Zn-III substrate DNA as sensors to detect M13 phage ssDNA

For each designed Zn-III substrate (S), about 5 pmol (excess) of the S and 1 pmol of the 7249-nt M13 genome (served as the programmed Zn-III enzyme strand) were mixed in 300 μl of the selection buffer (50 mM HEPES (pH 7.05 at 23°C), 100 mM NaCl, 5 mM $MgCl_2$ and 2 mM $ZnCl_2$). The mixture was undergone five rounds of thermal cycling (each round: 70°C for 2 min, then 37°C for 30 min) to promote deoxyribozyme multiple-turnovers (12). About 20 μl of bacterial cell lysate was doped into an experimental group to mimic a biological environment. After thermal cycling, the samples were precipitated with ethanol, resuspended in 20 μl of the loading buffer (90% formamide, 30 mM EDTA), and run into 15% denaturing PAGE gels for bands separation. The gels were stained by SYBR Gold, and scanned with a Bio-rad ChemiDoc MP Imaging System. Large pieces of DNA, including the 7249-nt M13, were stuck at the bottom of gel wells.

RESULTS AND DISCUSSION

Identification of the class III & IV deoxyribozymes with the new ssDNA library

The current (Cur) ssDNA library construct (149 nt) contains 100 random-sequence positions and is identical to the previous (Pre) one (10) except for the existence of the designed 11-bp terminal hybridization (29) to promote circularization by CircLigase (Figure 1 & Supplementary Figure S1, Supporting Information: sequence). For any synthetic DNA sequence library with over 25 random nucleotides, a typical usage of 10^{14} (~200 pmol) molecules for *in vitro* selection allows only a portion ($<10^{-1}$) of all possible sequence ($>4^{25} \approx 10^{15}$) to be interrogated. In our selection libraries, we set up the number of random nucleotides up to 100 in order to provide substantial structural possibilities for selection of deoxyribozymes that can use metal ion as a co-factor. As a consequence, merely a tiny portion ($\sim 10^{-46}$) of all possible DNA sequence ($4^{100} \approx 10^{60}$) can be examined by a typical *in vitro* selection (a usage of 10^{14} molecules). In fact, the practical nanomole amount (10^{15}–10^{18}) of DNA library that can be used to initiate an *in vitro* selection experiment is far behind and can never ever cover all sequence possibilities (10^{60}) of such library constructs.

Starting with the new library of $\sim 1.2 \times 10^{14}$ (~200 pmol in 100 μl) linear ssDNAs, we achieved a 78% yield of the CircLigase-catalyzed initial (G0) DNA circularization, which corresponds to a circa 2.4-fold improvement comparing to the 32% circularization efficiency with the previous library (Figure 1). However, considering that our selection faces a coverage deficit of 10^{-46}, a factor of only 2.4 may be slightly helpful in covering more of the sequence space. Nevertheless, with this improved G0 sequence pool of circular ssDNA, we continued the selection (10) for DNA-hydrolyzing DNAs in a buffer containing 50 mM HEPES (pH 7.05 at 23°C), 100 mM NaCl, 5 mM $MgCl_2$ and 2 mM $ZnCl_2$ at 37°C. Same selection pressure (e.g. shortening incubation time as the selection went on, bringing in mutagenic PCR to the later rounds of the selection, etc.) to the one used in the previous study (10) was applied here. After 9 rounds of selective amplification, the G9 DNA library exhibited a 10% signal of self-cleavage after 1 min of incubation, and was chosen for high-throughput sequencing.

In the previous study (10), high-throughput sequencing had also been conducted with the G9 population, wherein two classes (Zn-I & Zn-II) of Zn^{2+}-dependent deoxyribozymes were identified. Re-analysis of the old sequencing data (Supporting Information-Excel 1) reveals occupancies of 58.26% for Zn-I and 2.89% for Zn-II in the total 1,666,067 reads (Figure 2A). The rest of the data includes sequence that has been experimentally tested with no activity (36.96%) and sequence that has not been tested and classified (1.89%).

Unsurprisingly, Zn-I and Zn-II still occupy the majority of the re-selected G9 pool in the new sequencing data (79.35% for the former and 5.19% for the latter in the total 3,313,122 reads); besides them, however two new classes termed Zn-III (0.37% of the pool) and Zn-IV (12.31% of the pool) are uncovered by the re-selection (Figure 2B, Supporting Information-Excel 2). Members of Zn-III & IV share no mutual similarities in sequence and architectural features (Supplementary Figure S2). They are also distinct from Zn-I & II (10), without carrying any of the two's conserved elements. Using the conserved features (sequence and architecture validated later in Figure 4A) of Zn-III & IV, we searched through the old G9 high-throughput sequencing data (Supporting Information-Excel 1) and confirmed the absence of the two new classes of deoxyribozymes in the selected pool of the previous study (10). Besides that, direct

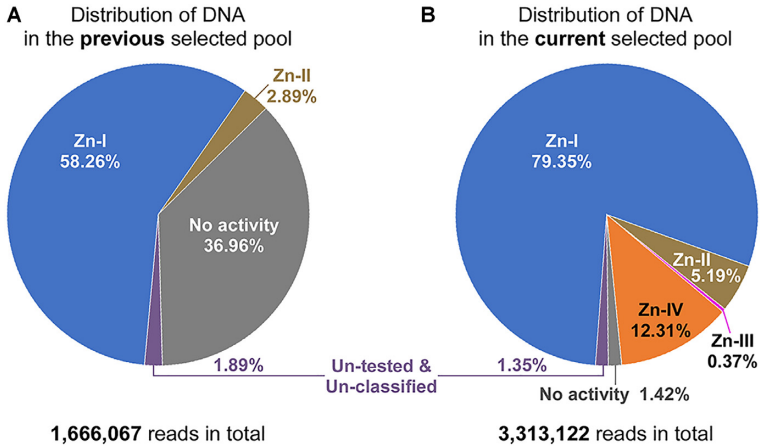

Figure 2. Distribution of DNA in the previous (**A**) and current (**B**) selected pools. Over a million reads from high-throughput sequencing of the G9 population were obtained for each selection. By searching the conserved features (sequence and secondary structure) of each class of deoxyribozyme (experimentally validated) through the sequencing data, their corresponding occupation rates were plotted into the pie charts. In both pools, there are certain levels of DNA that were tested without showing a catalytic activity (No activity). Less than 2% of each pool is un-tested & un-classified.

comparison of the DNA distribution in the previous (10) and current G9 pools reveals increased occupancies for both Zn-I & II and a greatly reduced portion of junk sequence (no activity) in the latter (Figure 2).

Interestingly, the predicted secondary structure by Mfold (32) (Supplementary Figure S2A) and the experimentally validated architecture (Figure 4A) reveal that in Zn-III the terminal hybridization stem serves as an integral part of its minimal catalytic structure. Thus the emergence of Zn-III from the current selection is highly likely due to the presence of that terminal stem in the new sequence library. In Zn-IV, the terminal hybridization stem seems rather far from the nucleotides that sustain its catalysis and does not appear to be a critical element to support its structure (Supplementary Figure S2B). Removal of the terminal stem also had negligible effects on Zn-IV's activity. Hence, the circa 2.4-fold improvement in sequence space coverage rather than the terminal structure itself contributes mainly to Zn-IV's emergence out of the current selection.

Characterization of the class III & IV DNA-hydrolyzing deoxyribozymes

After truncation, minimized DNA constructs of the two representatives (Zn-III-R1 & Zn-IV-R1) catalyze DNA hydrolysis at specific sites that are trait for the corresponding class (Figure 3A and B). By comparison with a synthetic DNA ladder on dPAGE, the cleavage site for each representative was pinpointed between the TpG dinucleotide. The resulting 5′ cleavage product migrated to the same position as of the corresponding marker DNA.

CircLigase circularizes ssDNA with a strict terminal requirement of 5′-PO_4 and 3′-OH. Only deoxyribozymes that hydrolyze the 3′ phosphoester bond generate such termini on the linearized ssDNA, and therefore can be selected by this strategy. Using exact mass spectrometry, the chemical groups on the cleaved termini of each deoxyribozyme was confirmed to be consistent with hydrolysis of the 3′ phosphoester of TpG, leaving 5′-PO_4 on G and 3′-OH on T (Figure 3C and D).

Besides hydrolysis, depurination and oxidative damage can also lead to DNA scission (33). In fact, DNA-cleaving deoxyribozymes functioning through these two mechanisms have been reported (34–35). However, scission of DNA by the two mechanisms causes the loss of one-base information at the cleavage site, leaving a decrease in total molecular weight of the DNA fragments and a non-OH group at the 3′ end of the 5′ cleavage fragment (Supplementary Figure S3). For Zn-III-R1 and Zn-IV-R1, according to the exact mass determined for their DNA products (Figure 3C and D), an increase (∼18 Da) but not decrease in total molecular weight after DNA cleavage completely rules out the possibility of DNA scission by depurination or oxidative damage. Indeed, the mass data matches well with the hydrolysis mechanism, in which a water molecule is split and joined to the cleavage products (Supplementary Figure S3).

To interrogate the conserved sequence and structure of Zn-III & IV, we performed a reselection with pools containing degenerate DNAs of the corresponding representatives (R1s) (Supplementary Figure S4). An early-stage population (G4) that underwent less selection pressure (1 h incubation) was picked up for high-throughput sequencing to establish the consensus sequence and secondary structure of the two classes (Figure 4A). Both classes exhibit a small catalytic core with ∼20 highly conserved and unique nucleotides. In Zn-III they are flanked by two nearby base-paired substructures (named P1 and P2 stem), while in Zn-IV the two flanking stems are more separate. Other distinctive features to discriminate Zn-III against Zn-IV include the much less conserved TpG dinucleotide at the cleavage site for the former. However, no matter how these two nucleotides mutated in Zn-III, the hydrolysis of DNA remained on the linkage between them (Supplementary Figure S5).

In addition, analysis of 30 clones from a late-stage population (G8) that experienced harsh re-selection stringency (5 min incubation, Supplementary Figure S4) revealed deoxyribozyme mutants with faster cleavage speeds (Figure 4B-D). For example, each of the two Zn-III mutants (R2&3)

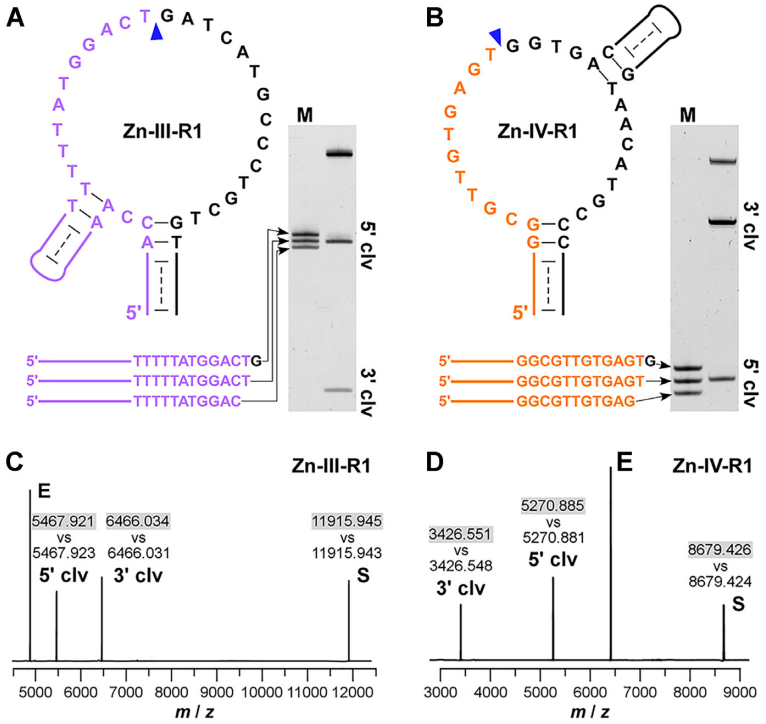

Figure 3. Identification of the class III & IV Zn^{2+}-dependent DNA-hydrolyzing deoxyribozymes. (**A, B**) Identified representatives (R1) of the class III & IV deoxyribozymes. Sequence and secondary structures are depicted on top-left. Cleavage sites are pointed out by arrowheads based on the comparison of the cleavage (clv) products with markers in dPAGE gels, which are shown on bottom-left. (**C, D**) Exact mass spectroscopic determination of the cleavage products of deoxyribozyme Zn-III-R1 and Zn-IV-R1. Note that truncated bimolecular constructs with an enzyme (**E**) strand cleaving a substrate (S) strand were used here (see Supporting Information: sequence for details). The proposed hydrolysis product peaks were annotated, with the calculated mass for hydrolysis of 3′ phosphoester bond shown on top and the observed mass at bottom.

contains 8 to 9 mutated bases around the catalytic core (Figure 4B). In the selection buffer with 2 mM $ZnCl_2$ at 37°C, they cleaved ∼2- to 3-fold faster than Zn-III-R1, with hydrolysis of DNA to nearly complete in 1 h for the most active deoxyribozyme Zn-III-R3. This corresponds to a k_{obs} value of 0.047 min^{-1} or a half-life of 15 min (Figure 4C). Similarly, 7 to 8 mutated bases were found in the mutants of Zn-IV (Figure 4B), with the best performer Zn-IV-R3 hydrolyzing at a k_{obs} of 0.051 min^{-1} or a half-life of 14 min (Figure 4D).

Apparently, Zn-III and Zn-IV dislike low reaction temperatures (both were identified through the selection at 37°C.). At 30°C, their cleavage speed was only one fifth of that at 37°C, while higher temperatures promoted their hydrolysis a bit (Figure 5A, Supplementary Figure S6). Removal of Mg^{2+} only from the selection buffer caused negligible effect on the hydrolysis activity of both classes (Supplementary Figure S7). Incubation of Zn-III-R3 and Zn-IV-R3 in reaction buffers containing a series of divalent metal ions further confirmed that the two classes of deoxyribozymes are Zn^{2+} dependent (Figure 5B). Also, both representatives have a narrow pH optimum near 7.05, with acceptable fluctuations of about ±0.10 unit (Figure 5C). Moreover, each of them robustly hydrolyzed DNA at the corresponding specific site with the concentration of Zn^{2+} cofactor at 2 mM. For Zn-IV-R3, even slight deviations from this optimum notably weakened its hydrolysis activity (Figure 5D).

Comparison of the four classes of Zn^{2+}-dependent DNA-hydrolyzing deoxyribozymes

The two classes of deoxyribozymes (Zn-III & Zn-IV) identified here behave very similar to the two previously reported classes (Zn-I & Zn-II) (10) in several aspects, including the sharp pH range (∼7) and Zn^{2+} concentration range (∼2 mM) (Figure 6), which is near the critical point of forming $Zn(OH)_2$/ZnO precipitation. At these conditions, it is believed that the polynuclear Zn^{2+} complexes generated in the solution act as the active species to promote DNA hydrolysis (13). Also all four classes favor high reaction temperatures, with improved k_{obs} beyond 37°C. However only Zn-I can maintain the overall high cleavage yield at high temperatures (12), while Zn-II, III, & IV generate less cleaved products when the temperature goes above 37°C. Therefore we recommend a reaction temperature of 37–45°C for Zn-I and 37°C for the rest three classes. In addition, the four classes all exhibit a clear feature of secondary structure, with a few unpaired nucleotides forming a loop region, wherein catalytic cleavage occurs. In a bimolecular construct, these unpaired nucleotides can be contributed by both DNA strands (Zn-I, II and IV) or mainly by one of the two strands (Zn-III) (Figure 6A). Usually, the loop is surrounded by the flanking one (Zn-I) or two stems (Zn-II, III and IV), which is similar to DNA-hydrolyzing DNAs identified by others (4–9). Among the four classes, Zn-I has the smallest 17-nt loop, with 15 nucleotides highly conserved; Zn-III and IV

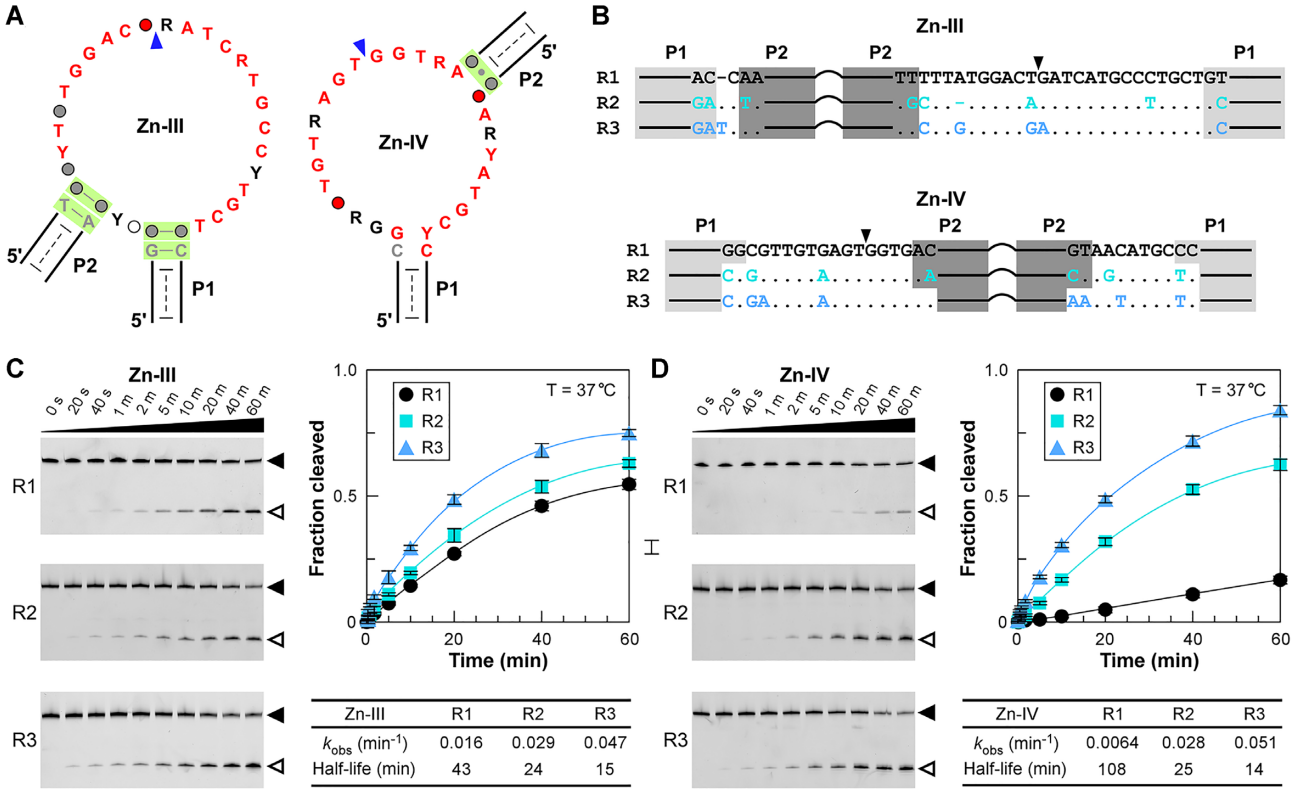

Figure 4. Reselection for active deoxyribozyme mutants. (**A**) Refined consensus sequence and secondary structure of Zn-III & IV. The refinement was based on high-throughput sequencing data of the 4th generation of a reselected library (Supplementary Figure S3). Nucleotides with conservation of at least 75%, 90% and 97% are shown in gray, black and red, respectively; less conserved nucleotides are represented by circles. Green shading denotes base pairs supported by covariation. R and Y denote purine and pyrimidine, respectively. Based-paired substructures (P1 & P2) are also pointed out. Arrowheads refer to the specific cleavage sites. (**B**) Comparison in sequence of the mutants to R1. Identical and missing nucleotides are shown as dots and dashes, respectively. Shadings in light and dark gray denote sequence that form P1 and P2, respectively. Arrowheads point to the cleavage sites. (**C, D**) Kinetic characterization of the representatives. In each panel, dPAGE gels reflecting the cleavage vs time are shown on the left; plot of the fraction of DNA cleaved vs time is depicted on the top right; the observed rate constant and half-life values are summarized on the bottom right. Filled and hollow arrowheads identify uncleaved DNA precursor and 5′-cleavage fragments, respectively. All of the gels were repeated at least twice with consistent results. The standard deviation in (C) and (D) was generated from three replicate assays.

have loops (∼25 nt in total, 20 highly conserved) larger than Zn-I but smaller than Zn-II (32 nt in total, 25 highly conserved). Interestingly, their catalytic speed seems to be negative correlated to the loop size, with the k_{obs} value (0.013 min^{-1}) of Zn-II about one-fourth of that of Zn-III (0.047 min^{-1}) and IV (0.051 min^{-1}) and one-eightieth of that of Zn-I (1 min^{-1}) (Figure 6B). However, reselection on Zn-II has not been reported. It is possible that with mutations in the loop the activity of Zn-II can be improved.

Zn-I can efficiently cleave a substrate DNA encompasses the seven particular nucleotides GTTGR∧AG, or 1 out of every 8192 (2×4^6) arbitrarily chosen DNA sites (Figure 6). In terms of the generality for site-specific DNA hydrolysis, it is the best among the four classes but poorer than the reported DNA-cleaving deoxyribozyme 10MD5 mutants (9), in which only two particular nucleotide identities at the cleavage site is required. Comparatively, Zn-III & IV have much poorer generality, requiring the recognition of over ten particular nucleotides in the substrate for hydrolysis, with the former being an extreme case, in which all (∼20) highly conserved nucleotides dwelling on the substrate (Figure 6).

Nucleotide identities in the stem region of the known DNA-hydrolyzing deoxyribozymes (4–10,14), including the Zn-I to IV, are generally less important, meaning that sequence in their stems is mostly programmable. Therefore after hydrolysis, Zn-I can generate customized ssDNA (the 3′ cleaved fragment) carrying only two scar (the highly conserved AG) nucleotides at the 5′ end, while Zn-II can help produce customized ssDNA (the 5′ cleaved fragment) with only one scar (the conserved G) nucleotide at the 3′ end (Figure 6A). Combinatorial usage of the two classes should allow the production of ssDNA with sequence customizable in all nucleotide positions except three (two at the 5′ and one at the 3′ end) (15). Comparing to Zn-I & II, the specific hydrolysis sites of Zn-III & IV are more into their loop region, thus generating more scars at the ends of the cleaved fragments (Figure 6).

Engineering DNA-responsive DNA hydrolyzers in Zn-III construction for DNA detection

The poor generality of Zn-III & IV for site-specific DNA hydrolysis limits their potential applications as therapeu-

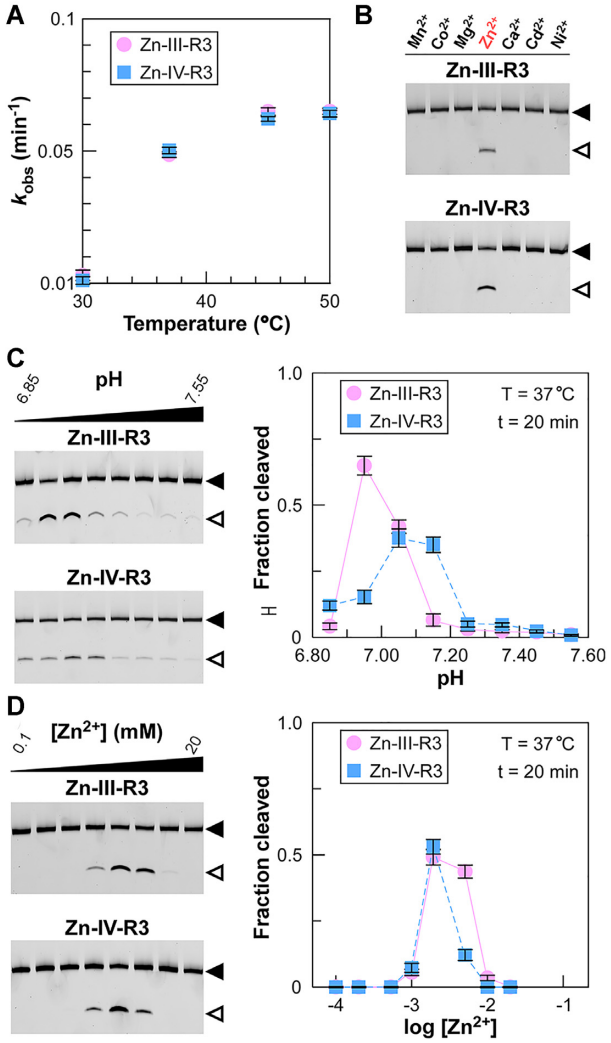

Figure 5. Temperature, metal ion, and pH dependence of Zn-III & IV deoxyribozymes. (**A**) k_{obs} versus temperature for the most active representatives (R3) of the two classes. Data was extracted from assays in Supplementary Figure S5. (**B**) Analysis of the activity of Zn-III-R3 and Zn-IV-R3 with other divalent metal ions. Samples were incubated with 2 mM of the ions for 30 min before separated by dPAGE. (**C, D**) Analysis of pH and $[Zn^{2+}]$ dependence of the two representative deoxyribozymes, respectively. Filled and hollow arrowheads identify uncleaved DNA precursor and 5′-cleavage fragments, respectively. All of the gels were repeated at least twice with consistent results. The standard deviation in (A), (C) and (D) was generated from three replicate assays.

tic tools for intracellular DNA cleavage, an aspect that has been demonstrated on the RNA side (36–37) with the RNA-cleaving deoxyribozymes (38–43) based on their broad generality. In fact, Zn-III has the poorest substrate generality among all known DNA-hydrolyzing deoxyribozymes (4–10). In a bimolecular construct, the highly conserved nucleotides (red, 20 nts) in this class all dwell on the substrate (S) DNA (Figure 6A and 7A). However, on the other hand, this extremeness of conserved sequence in one DNA strand leads to the unusual great generality of the other, that is, the great generality of the enzyme (E) DNA (Figures 6A and 7A).

For all known DNA-hydrolyzing deoxyribozymes (4–10), nucleotides in their stem region, especially those away from the catalytic loop in the secondary structure, are generally programmable under the premise of maintaining the base complementation. By point mutations and covariations on Zn-III-R2 (Figure 7A), we further confirmed that nucleotide identities in the first base pairs of stems P1 and P2 that hold up the catalytic loop had no effect on cleavage efficiency, hinting that in Zn-III-R2 the entire P1 and P2 stems are very likely programmable. Thus Zn-III-R2 presumably uses some or all of the ∼20 conserved nucleotides on the S strand as part of its catalytic mechanism, considering that aside from the single unpaired nucleotide in the E strand, all 'enzyme' nucleotides are part of base-pairing (P1 and P2 stems) and therefore unlikely to participate in catalysis. Certain levels of conservation appeared on the single-nucleotide bulge (marked with an asterisk, preference: C>T>A>G, nearly an order of magnitude of difference in the observed cleavage yield between C and G) in the E strand (Figure 7A). Taking all these into account, it is reasonable to believe that Zn-III-R2 owns unique broad generality on its E strand, with the requirement of merely one particular nucleotide identity at the bulge position, even which might be negligible if less active hydrolysis is tolerable for the potential downstream applications.

We explored this uniqueness of Zn-III to engineer DNA-responsive DNA hydrolyzers for DNA detection. By treating a target (7249-nt M13 phage genome) ssDNA segment as the E strand of Zn-III, we were able to design a corresponding S strand of Zn-III to match up with the E through Watson–Crick base pairing for target-DNA-triggered cleavage of the S (Figure 7B). Due to the broad sequence-generality of the E in Zn-III, in principle the S strand can be programmed to sense any sequence with more than a dozen of nucleotides as an E strand in the Zn-III fashion. The length requirement is mainly to guarantee the formation of stable P1 and P2 stems in the engineered Zn-III construct to support the hydrolysis. As a proof of principle, we randomly chose two segments (E1&2) in M13 as the targets, and showed that the corresponding designed Zn-III S (S1 and S2) strands can be site-specifically cleaved when M13 and the S were mixed together under the deoxyribozyme reaction conditions (Figure 7B). In the process of designing the S according to the E's sequence, we intentionally left a cytosine on the single-nucleotide bulge position of the E when the S was targeted by the E through Watson–Crick base pairing. By doing so, we ensured the high cleavage efficiency of Zn-III and were able to detect the cleaved S fragments by the gel-based assay. This approach might be unnecessary if more sensitive detection methods, e.g., isothermal amplification-based methods (44–52), were combined to monitor the ssDNA cleavage event. In addition, it is worthy to note that as a sensor the S of Zn-III can only be triggered by a DNA but not RNA target strand (Supplementary Figure S8).

CONCLUSIONS

Simply by programming a terminal hybridization stem in the sequence library, we were able to discover two new

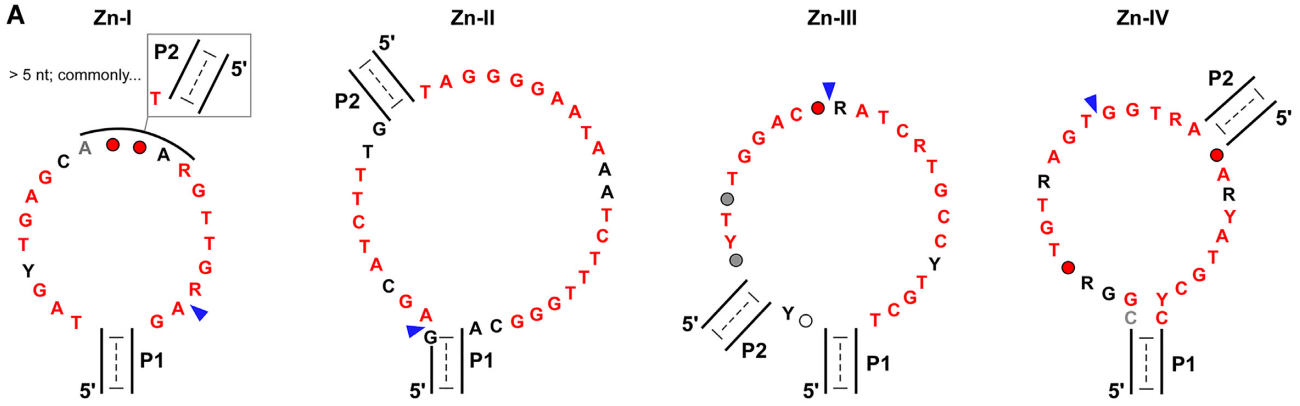

B

Class	pH	Saturated [Zn^{2+}]	Saturated rate at 37 °C	Half-life at 37 °C	Recommended temperature	Substrate requirement	Features of the cleavage
I	6.95–7.05	1–2 mM	1.0 min^{-1}	42 sec	37–45 °C	5'-GTTGR^AG	Robust hydrolysis, generating a 3' fragment with only two scar bases (AG) left on the 5' end
II	6.95–7.05	1–2 mM	0.013 min^{-1}	53 min	37 °C	5'-G^AGCATCTTTGGC	Relatively slow hydrolysis, leaving only a scar base (G) at the 3' end of the 5' fragment
III	6.95–7.00	2–5 mM	0.047 min^{-1}	15 min	37 °C	5'-YTTGGACN^RATCR TGCCYTGCT	Hydrolysis at a medium speed, with the highly conserved bases accumulated on the to-be-cleaved loop, yielding a bunch of scars at the ends of the cleaved fragments
IV	7.05–7.15	2 mM	0.051 min^{-1}	14 min	37 °C	5'-GGRNTGTRAGT^G GTRA	Hydrolysis at a medium speed, yielding five scar bases (GGTRA) at the 5' end of the 3' fragment

Figure 6. Comparison of the class I–IV Zn^{2+}-dependent DNA-hydrolyzing deoxyribozymes. (**A**) Comparison in consensus sequence and secondary structure. Models for Zn-I and Zn-II were re-drawn according to Ref. 10 and 12 with permissions. Models for Zn-III and Zn-IV were generated by this study. Note that the re-selection on Zn-II has not been reported. Therefore its current model was built on the original sequencing data on the selection of a 145-nt ssDNA library in Ref. 10. Nucleotides with conservation of at least 75%, 90% and 97% are shown in gray, black and red, respectively; less conserved nucleotides are represented by circles. R and Y denote purine and pyrimidine, respectively. Based-paired substructures (P1 & P2) are also pointed out. Arrowheads refer to the specific cleavage sites. (**B**) A summary of the class I–IV Zn^{2+}-dependent DNA-hydrolyzing deoxyribozymes. The information was extracted from (10) and (12) as well as this study. Sequence shown in the column of Substrate requirement refers to the essential nucleotides on an ssDNA substrate. ∧ refers to the cleavage site. N denotes random nucleotide. Note that besides the essential nucleotides, more and programmable nucleotides are required at the 5′ and 3′ ends of the substrate DNA to allow the formation of the flanking base-complementation with the enzyme strand for cleavage in a bimolecular construct.

classes (Zn-III and Zn-IV) of DNA-hydrolyzing DNAs with an old CircLigase-based selection strategy (10). For the selection, the benefit from a terminal hybridization stem is believed to be twofold: it provides a pre-existing substructure to enhance the library's functional potential, a similar scenario that has been seen on the selection of aptamers previously (30); meanwhile, it also promotes the circularization of ssDNA (29) to expand the library's effective sequence capacity, though such promotion seems to be slight. The secondary structure of the uncovered deoxyribozymes indicates that the terminal stem directly facilitates the evolution of Zn-III by serving as a critical structural element to support this class's catalysis. In a bimolecular construct, Zn-III exhibits broad sequence-generality on the enzyme strand, which could be harnessed to engineer DNA-responsive DNA hydrolyzers for detection of any target ssDNA sequence.

It should be noted that the CircLigase-based selection strategy includes two steps (steps i and v, Figure 1) of circularization in each round of selection (10). While the terminal hybridization stem promotes the ligation efficiency in the first step (step i), in principle it has nothing to do for the second (step v). Hence, there may be still room to further optimize the selection by tackling the potential ligation-efficiency issue in the second step in the future.

With the improved approach for CircLigase-based selection, we plan to resume searching for DNA-hydrolyzing DNAs that depend on other metal ions. We expect that new types of hydrolytic DNAs will be continuously identified, and the expanding repertoire of deoxyribozymes will stimulate the development of molecular biology, DNA biotechnology, as well as other DNA-technology-relevant fields.

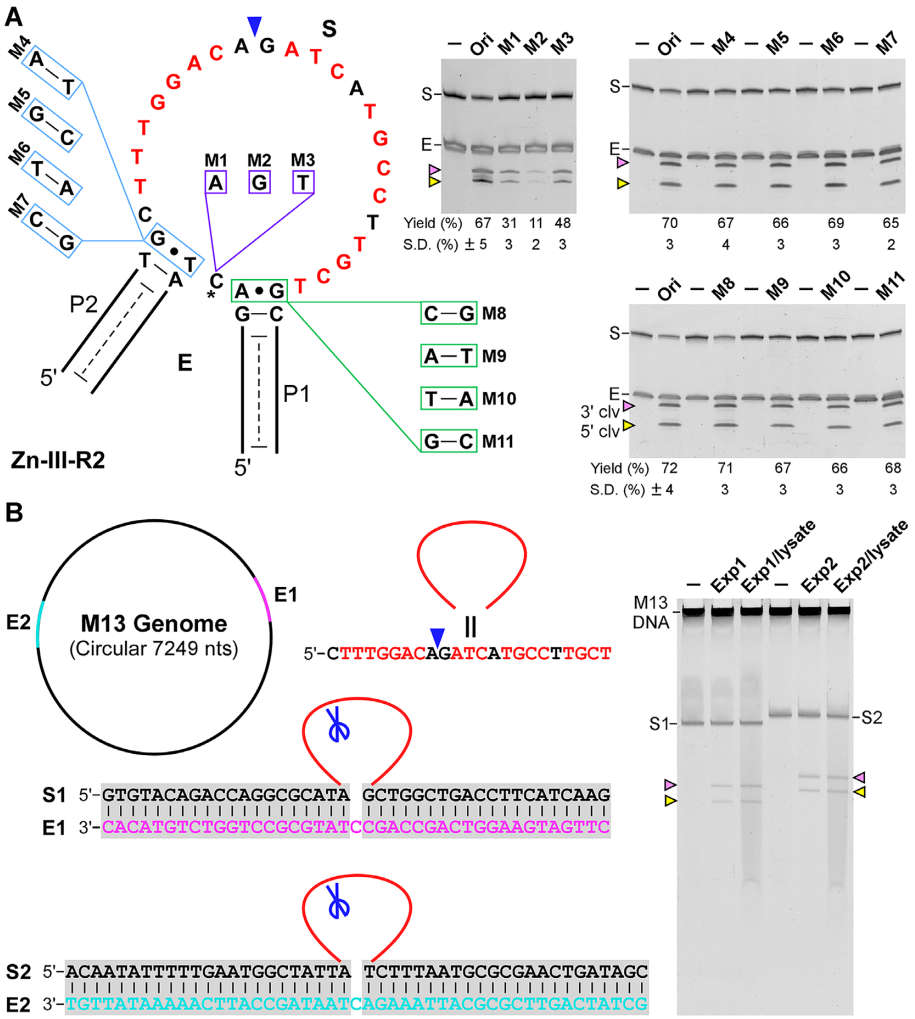

Figure 7. Programming Zn-III for potential DNA detection. (**A**) Mutational studies to investigate the sequence-programmability of the E strand in Zn-III. All reaction samples were incubated with Zn^{2+} at 37°C for 1 h. The unreacted samples (−) and original (Ori) Zn-III-R2 were used as controls in dPAGE. The 5′ and 3′ cleaved fragments were pointed out by yellow and pink arrowheads, respectively. All of the assays were repeated three times with consistent results. Yields were listed at the bottom of the gels, with the standard deviation generated from three replicate assays. (**B**) Engineering Zn-III substrate (S) strands to sense M13 genome. Two randomly-chosen segments (E1&2) in M13 were treated as the enzyme (E) strands of Zn-III, leading to the design of the corresponding Zn-III substrate (S1 and S2) strands. Cleavage of the S strands was observed in the experimental (Exp) groups when M13 and the S were mixed under the deoxyribozyme reaction conditions, including in the ones with bacterial cell lysate supplemented to mimic a biological environment. The mixture of M13 and the S with the absence of Zn^{2+} was used as a control (−).

DATA AVAILABILITY

All data included in this study is available upon request by contact with the corresponding author.

SUPPLEMENTARY DATA

Supplementary Data are available at NAR Online.

FUNDING

National Key Research and Development Program of China [2020YFA0908901]; National Natural Science Foundation of China [91859104, 81861138004, 21673050]. Funding for open access charge: National Natural Science Foundation of China.

Conflict of interest statement. Authors declare the following competing financial interests: two China patents on the sequence and secondary structure of Zn-III & IV deoxyribozymes have been filed.

REFERENCES

1. Srinivasan,J., Cheatham,T.E., Cieplak,P., Kollman,P.A. and Case,D.A. (1998) Continuum solvent studies of the stability of DNA, RNA, and phosphoramidate - DNA helices. *J. Am. Chem. Soc.*, **120**, 9401–9409.
2. Williams,N.H., Takasaki,B., Wall,M. and Chin,J. (1999) Structure and nuclease activity of simple dinuclear metal complexes: quantitative dissection of the role of metal ions. *Acc. Chem. Res*, **32**, 485–493.
3. Schroeder,G.K., Lad,C., Wyman,P., Williams,N.H. and Wolfenden,R. (2006) The time required for water attack at the phosphorus atom of simple phosphodiesters and of DNA. *Proc. Natl. Acad. Sci. U.S.A.*, **103**, 4052–4055.
4. Chandra,M., Sachdeva,A. and Silverman,S.K. (2009) DNA-catalyzed sequence-specific hydrolysis of DNA. *Nat. Chem. Biol.*, **5**, 718–720.
5. Xiao,Y., Chandra,M. and Silverman,S.K. (2010) Functional compromises among pH tolerance, site specificity, and sequence

tolerance for a DNA-hydrolyzing deoxyribozyme. *Biochemistry*, **49**, 9630–9637.
6. Xiao,Y., Allen,E.C. and Silverman,S.K. (2011) Merely two mutations switch a DNA-hydrolyzing deoxyribozyme from heterobimetallic (Zn2+/Mn2+) to monometallic (Zn2+-only) behavior. *Chem. Commun.*, **47**, 1749–1751.
7. Dokukin,V. and Silverman,S.K. (2012) Lanthanide ions as required cofactors for DNA catalysts. *Chem. Sci*, **3**, 1707–1714.
8. Velez,T.E., Singh,J., Xiao,Y., Allen,E.C., Wong,O.Y., Chandra,M., Kwon,S.C. and Silverman,S.K. (2012) Systematic evaluation of the dependence of deoxyribozyme catalysis on random region length. *ACS Comb. Sci.*, **14**, 680–687.
9. Xiao,Y., Wehrmann,R. J., Ibrahim,N. A. and Silverman,S.K. (2012) Establishing broad generality of DNA catalysts for site-specific hydrolysis of single-stranded DNA. *Nucleic Acids Res.*, **40**, 1778–1786.
10. Gu,H., Furukawa,K., Weinberg,Z., Berenson,D.F. and Breaker,R.R. (2013) Small, highly active DNAs that hydrolyze DNA. *J. Am. Chem. Soc.*, **135**, 9121–9129.
11. Dhamodharan,V., Kobori,S. and Yokobayashi,Y. (2017) Large scale mutational and kinetic analysis of a self-hydrolyzing deoxyribozyme. *ACS Chem. Biol.*, **12**, 2940–2945.
12. Du,X., Zhong,X., Li,W., Li,H. and Gu,H. (2018) Retraining and optimizing DNA-hydrolyzing deoxyribozymes for robust single- and multiple-turnover activities. *ACS Catal.*, **8**, 5996–6005.
13. Moon,W.J., Yang,Y. and Liu,J. (2021) Zn^{2+}-dependent DNAzymes: from solution chemistry to analytical, materials and therapeutic applications. *ChemBioChem*, **22**, 779–789.
14. Gu,H. and Breaker,R.R. (2013) Production of single-stranded DNAs by self-cleavage of rolling-circle amplification products. *BioTechniques*, **54**, 337.
15. Praetorius,F., Kick,B., Behler,K.L., Honemann,M.N., Weuster-Botz,D. and Dietz,H. (2017) Biotechnological mass production of DNA origami. *Nature*, **552**, 84–87.
16. Wang,J., Wang,H., Wang,H., He,S., Li,R., Deng,Z., Liu,X. and Wang,F. (2019) Nonviolent self-catabolic DNAzyme nanosponges for smart anticancer drug delivery. *ACS Nano*, **13**, 5852–5863.
17. Alon,D.M., Voigt,C.A. and Elbaz,J. (2020) Engineering a DNAzyme-based operon system for the production of DNA nanoscaffolds in living bacteria. *ACS Synth. Biol.*, **9**, 236–240.
18. Furukawa,K. and Minakawa,N. (2014) Allosteric control of a DNA-hydrolyzing deoxyribozyme with short oligonucleotides and its application in DNA logic gates. *Org. Biomol. Chem.*, **12**, 3344–3348.
19. Xu,J., Sun,Y., Sheng,Y., Fei,Y., Zhang,J. and Jiang,D. (2014) Engineering a DNA-cleaving DNAzyme and PCR into a simple sensor for zinc ion detection. *Anal. Bioanal. Chem.*, **406**, 3025–3029.
20. Endo,M., Takeuchi,Y., Suzuki,Y., Emura,T., Hidaka,K., Wang,F., Willner,I. and Sugiyama,H. (2015) Single-molecule visualization of the activity of a Zn(2+)-dependent DNAzyme. *Angew. Chem. Int. Ed.*, **54**, 10550–10554.
21. Lilienthal,S., Shpilt,Z., Wang,F., Orbach,R. and Willner,I. (2015) Programmed DNAzyme-triggered dissolution of DNA-based hydrogels: means for controlled release of biocatalysts and for the activation of enzyme cascades. *ACS Appl. Mater. Interfaces*, **7**, 8923–8931.
22. Silverman,S.K. (2016) Catalytic DNA: scope, applications, and biochemistry of deoxyribozymes. *Trends Biochem. Sci.*, **41**, 595–609.
23. Engelhardt,F.A.S., Praetorius,F., Wachauf,C.H., Bruggenthies,G., Kohler,F., Kick,B., Kadletz,K.L., Pham,P.N., Behler,K.L., Gerling,T. *et al.* (2019) Custom-size, Functional, and durable DNA origami with design-specific scaffolds. *ACS Nano*, **13**, 5015–5027.
24. Ma,L. and Liu,J. (2020) Catalytic nucleic acids: biochemistry, chemical biology, biosensors, and nanotechnology. *iScience*, **23**, 100815.
25. Li,X., Ding,X., Li,Y., Wang,L. and Fan,J. (2016) A TiS2 nanosheet enhanced fluorescence polarization biosensor for ultra-sensitive detection of biomolecules. *Nanoscale*, **8**, 9852–9860.
26. Liu,N., Hou,R., Gao,P., Lou,X. and Xia,F. (2016) Sensitive Zn(2+) sensor based on biofunctionalized nanopores via combination of DNAzyme and DNA supersandwich structures. *Analyst*, **141**, 3626–3629.
27. Li,H., Wang,M., Shi,T., Yang,S., Zhang,J., Wang,H.H. and Nie,Z. (2018) A DNA-mediated chemically induced dimerization (D-CID) nanodevice for nongenetic receptor engineering to control cell behavior. *Angew. Chem. Int. Ed.*, **57**, 10226–10230.
28. Xiong,Q., Xie,C., Zhang,Z., Liu,L., Powell,J.T., Shen,Q. and Lin,C. (2020) DNA origami post-processing by CRISPR-Cas12a. *Angew. Chem. Int. Ed.*, **59**, 3956–3960.
29. Li,Q., Zhang,S., Li,W., Ge,Z., Fan,C. and Gu,H. (2021) Programming CircLigase catalysis for DNA rings and topologies. *Anal. Chem.*, **93**, 1801–1810.
30. Ruff,K.M., Snyder,T.M. and Liu,D.R. (2010) Enhanced functional potential of nucleic acid aptamer libraries patterned to increase secondary structure. *J. Am. Chem. Soc.*, **132**, 9453–9464.
31. Breaker,R.R. and Joyce,G.F. (1994) Inventing and improving ribozyme function - rational design versus iterative selection methods. *Trends Biotechnol.*, **12**, 268–275.
32. Zuker,M. (2003) Mfold web server for nucleic acid folding and hybridization prediction. *Nucleic Acids Res.*, **31**, 3406–3415.
33. Lindahl,T. (1993) Instability and decay of the primary structure of DNA. *Nature*, **362**, 709–715.
34. Sheppard,T.L., Ordoukhanian,P. and Joyce,G.F. (2000) A DNA enzyme with N-glycosylase activity. *P. Natl. Acad. Sci.*, **97**, 7802–7807.
35. Carmi,N., Shultz,L.A. and Breaker,R.R. (1996) In vitro selection of self-cleaving DNAs. *Chem. Biol.*, **3**, 1039–1046.
36. Dass,C.R., Choong,P.F.M. and Khachigian,L.M. (2008) DNAzyme technology and cancer therapy: cleave and let die. *Mol. Cancer Ther.*, **7**, 243–251.
37. Khachigian,L.M. (2019) Deoxyribozymes as catalytic nanotherapeutic agents. *Cancer Res.*, **79**, 879–888.
38. Santoro,S.W. and Joyce,G.F. (1997) A general purpose RNA-cleaving DNA enzyme. *P. Natl. Acad. Sci.*, **94**, 4262–4266.
39. Torabi,S.F., Wu,P., McGhee,C.E., Chen,L., Hwang,K., Zheng,N., Cheng,J. and Lu,Y. (2015) In vitro selection of a sodium-specific DNAzyme and its application in intracellular sensing. *Proc. Natl. Acad. Sci. U.S.A.*, **112**, 5903–5908.
40. Saran,R. and Liu,J. (2016) A Silver DNAzyme. *Anal. Chem.*, **88**, 4014–4020.
41. Zhou,W., Saran,R., Chen,Q., Ding,J. and Liu,J. (2016) A new Na(+)-dependent RNA-cleaving DNAzyme with over 1000-fold rate acceleration by ethanol. *ChemBioChem*, **17**, 159–163.
42. Zhou,W., Zhang,Y., Huang,P., Ding,J. and Liu,J. (2016) A DNAzyme requiring two different metal ions at two distinct sites. *Nucleic Acids Res.*, **44**, 354–363.
43. Saran,R., Kleinke,K., Zhou,W., Yu,T. and Lee,J.W. (2017) A silver-specific DNAzyme with a new silver aptamer and salt-promoted activity. *Biochemistry*, **56**, 1955–1962.
44. Notomi,T., Okayama,H., Masubuchi,H., Yonekawa,T., Watanabe,K., Amino,N. and Hase,T. (2000) Loop-mediated isothermal amplification of DNA. *Nucleic Acids Res.*, **28**, e63.
45. Vincent,M., Xu,Y. and Kong,H. (2004) Helicase-dependent isothermal DNA amplification. *Embo. Rep*, **5**, 795–800.
46. Piepenburg,O., Williams,C.H., Stemple,D.L. and Armes,N.A. (2006) DNA detection using recombination proteins. *Plos. Biol.*, **4**, 1115–1121.
47. Daher,R.K., Stewart,G., Boissinot,M. and Bergeron,M.G. (2016) Recombinase polymerase amplification for diagnostic applications. *Clin. Chem.*, **62**, 947–958.
48. Gootenberg,J.S., Abudayyeh,O.O., Lee,J.W., Essletzbichler,P., Dy,A.J., Joung,J., Verdine,V., Donghia,N., Daringer,N.M., Freije,C.A. *et al.* (2017) Nucleic acid detection with CRISPR-Cas13a/C2c2. *Science*, **356**, 438.
49. Chen,J.S., Ma,E.B., Harrington,L.B., Da Costa,M., Tian,X.R., Palefsky,J.M. and Doudna,J.A. (2018) CRISPR-Cas12a target binding unleashes indiscriminate single-stranded DNase activity. *Science*, **360**, 436–439.
50. Gootenberg,J.S., Abudayyeh,O.O., Kellner,M.J., Joung,J., Collins,J.J. and Zhang,F. (2018) Multiplexed and portable nucleic acid detection platform with Cas13, Cas12a, and Csm6. *Science*, **360**, 439–444.
51. Harrington,L.B., Burstein,D., Chen,J.S., Paez-Espino,D., Ma,E., Witte,I.P., Cofsky,J.C., Kyrpides,N.C., Banfield,J.F. and Doudna,J.A. (2018) Programmed DNA destruction by miniature CRISPR-Cas14 enzymes. *Science*, **362**, 839.
52. Li,J., Macdonald,J. and von Stetten,F. (2019) Review: a comprehensive summary of a decade development of the recombinase polymerase amplification. *Analyst*, **144**, 31–67.